3D-Electrode Architectures for Enhanced Direct Bioelectrocatalysis of Pyrroloquinoline Quinone-Dependent Glucose Dehydrogenase

David Sarauli,*,[†] Kristina Peters,[‡] Chenggang Xu,[§] Burkhard Schulz,[||] Dina Fattakhova-Rohlfing,[‡] and Fred Lisdat*,[†]

[†]Biosystems Technology, Institute for Applied Life Sciences, Technical University of Applied Sciences Wildau, Hochschulring 1, D-15745 Wildau, Germany

[‡]Department of Chemistry and Centre for NanoScience (CeNS), University of Munich (LMU), Butenandtstraße 5–13 (E), D-81377, Munich, Germany

[§]UP Transfer GmbH, Am Neuen Palais 10, D-14469 Potsdam, Germany

[||]Institute for Chemistry, University of Potsdam, Karl-Liebknecht-Straße 24–25, D-14476 Potsdam, Germany

ABSTRACT: We report on the fabrication of a complex electrode architecture for efficient direct bioelectrocatalysis. In the developed procedure, the redox enzyme pyrroloquinoline quinone-dependent glucose dehydrogenase entrapped in a sulfonated polyaniline [poly(2-methoxyaniline-5-sulfonic acid)-co-aniline] was immobilized on macroporous indium tin oxide (macroITO) electrodes. The use of the 3D-conducting scaffold with a large surface area in combination with the conductive polymer enables immobilization of large amounts of enzyme and its efficient communication with the electrode, leading to enhanced direct bioelectrocatalysis. In the presence of glucose, the fabricated bioelectrodes show an exceptionally high direct bioelectrocatalytical response without any additional mediator. The catalytic current is increased more than 200-fold compared to planar ITO electrodes. Together with a high long-term stability (the current response is maintained for >90% of the initial value even after 2 weeks of storage), the transparent 3D macroITO structure with a conductive polymer represents a valuable basis for the construction of highly efficient bioelectronic units, which are useful as indicators for processes liberating glucose and allowing optical and electrochemical transduction.

KEYWORDS: 3D electrode structures, macroITO, conductive polymer, PQQ-GDH, direct bioelectrocatalysis, bioelectrochemistry
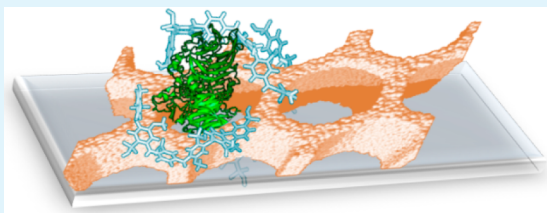
INTRODUCTION

The fabrication of electronic devices based on biological units is a very attractive and an intensively explored concept because it offers the possibility of benefitting from extremely high efficiencies and selectivities of biological systems optimized by nature. Successful examples of such technologies include enzyme-based bioelectrochemical devices such as biosensors, biofuel cells, and bioelectronics devices, which were already fabricated for a number of biomolecules.[1−7] A key for the electrochemical device functionality is the electronic communication between the electrode and an enzyme, which require proper design of the electrode architecture. The composition and morphology of the electrode layers are particularly important; equally essential is how the bioentities are bound to the electrodes without any deterioration of their biological functionality.[8−11]

Primarily highly conductive materials such as modified graphite or metals have been utilized as electrodes for the binding of redox biomolecules. However, these surfaces often produce an unwanted orientation of immobilized bioentities. Moreover, the nontransparent electrodes are not suitable for photoelectrochemical applications requiring interaction with light, as well as for fundamental spectroelectrochemical studies. In this context, transparent conducting oxides (TCOs), such as

tin-doped indium oxide (ITO)[12−16] or other doped tin oxides,[17−21] have emerged as intensively used electrodes for bioelectrochemical applications. Besides the common planar geometries, TCO electrodes with controlled porous architectures have received growing attention as alternative electrode materials for enzyme immobilization.[22−28] The interest in 3D-porous electrodes is caused by their large surface area and an accessible conducting interface enabling the incorporation of large amounts of active species and their direct communication with the electrode.

Porous TCO electrodes have been successfully applied for the immobilization of various redox moieties. The reported examples include electrochemiluminescent dyes demonstrating more than 2 orders of magnitude higher electroluminescence intensity on porous electrodes compared to the planar ones.[29] Furthermore, redox proteins, such as cytochrome c (cyt c),[24,28,30−32] ferredoxin,[33] hemoglobin,[26] and azurin,[31] were successfully incorporated into porous TCO electrodes with a very high loading related to the specific surface area of the porous electrode. So far, however, the advantages offered by

porous TCO electrodes could be demonstrated only for relatively small biological species. Bulkier biological entities, such as the majority of the practically relevant enzymes, or more complex systems based on polymer-embedded enzymes were practically not investigated, and a few reported systems did not show the expected increase in the electrochemical activity.[19,34] The major reasons for that are either the small pore size of the used TCO electrodes, making them inaccessible for the large species, or the poor communication between the incorporated enzyme and the electrode.

In this report, we demonstrate the clearly enhanced direct bioelectrocatalysis of the redox enzyme pyrroloquinoline quinone-dependent glucose dehydrogenase (PQQ-GDH) fixed by a sulfonated polyaniline copolymer (PMSA1) on macroporous ITO electrodes. This enzyme is insensitive to the oxygen level in the sample and exhibits high catalytic activity at physiological pH; hence, it represents an interesting bioentity for the engineering of biocatalytic glucose sensors.[7,35−37] Moreover, biocatalytic electrodes made of carbon nanotube materials modified with PQQ-GDH have already been applied in biofuel cells effectively operating in physiological media.[38−41] Recently, we demonstrated the ability of sulfonated polyaniline copolymer containing 2-methoxyaniline-5-sulfonic acid and aniline monomers not only to react directly with PQQ-GDH[42] but also to serve as a matrix without inhibiting the catalytic activity of the entrapped enzyme on gold and planar ITO electrodes.[43] In this study, we introduce a new system by exploiting the polymer/enzyme interaction and combining both compounds with the highly porous 3D structure of macroporous ITO electrodes while ensuring a high enzyme activity and an efficient bioelectrocatalysis in the presence of glucose.

■ RESULTS AND DISCUSSION

Fabrication and Characterization of macroITO and macroITO/(PMSA1:PQQ-GDH) Electrodes. The principle of the used electrodes is depicted in Scheme 1. Because the

Scheme 1. Principle of the Used Electrode Architecture
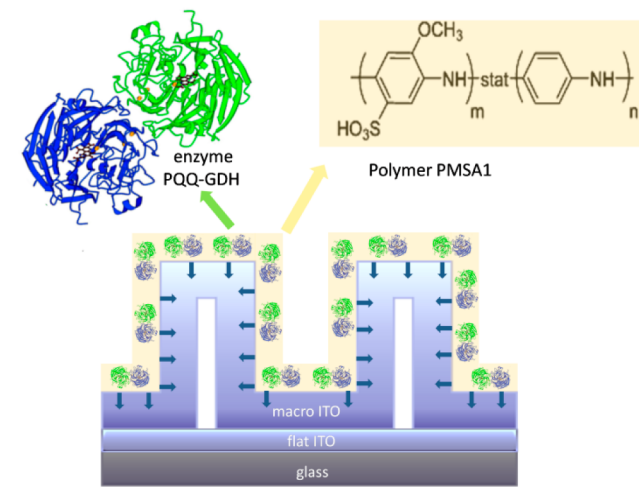
accessibility of the electrode surface in 3D structures can limit the bioelectrochemical performance, we intended to use a porous ITO scaffold with sufficiently large pore size to allow the efficient transport of polymer and enzyme during the preparation but also to not limit the transport of the enzyme substrate into the 3D electrode during operation. For this

purpose, we have composed our electrodes by the deposition of macroITO layers on top of commercial flat ITO substrates. The thickness of the porous ITO layer is about 1.2 μm after calcination. Scanning electron microscopy (SEM) and transmission electron microscopy (TEM) of these coatings reveal their homogeneous and crack-free morphology with a uniform pore structure composed of ca. 300 nm interconnected spherical pores (Figure 1A). The electrical conductivity of the porous ITO scaffold is 4.0 ± 0.3 S cm^{-1} after annealing in a forming-gas atmosphere at 400 °C.[26]
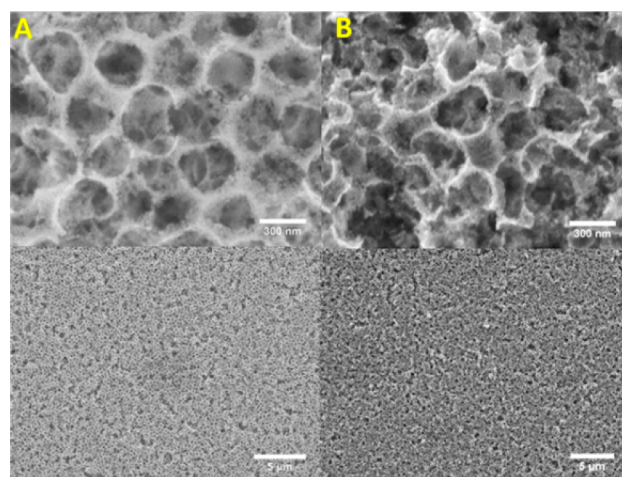
Figure 1. Top view of SEM images of (A) blank macroITO and (B) macroITO/(PMSA1:PQQ-GDH) films.

The sulfonated polyaniline copolymer PMSA1 has already been shown to react efficiently with PQQ-GDH.[42] Because of its good biocompatibility, it can also serve as a matrix, in which PQQ-GDH can be entrapped without loss of the catalytic activity. Both arguments are used here as starting points for the study of this system on macroITO electrodes (Scheme 1). Figure 1B demonstrates the morphology of macroITO electrodes after the polymer and enzyme are allowed to deposit within the structure. It can be seen that the porosity and homogeneity are not damaged upon polymer and enzyme functionalization of the films even under current flow through the system.

As a further confirmation, cyclic voltammetry of the polymer/enzyme-coated electrodes has been performed. It can be seen that the blank macroITO electrode does not show any redox transformation (Figure 2A, curve 1). After immobilization of PMSA1 alone (Figure 2A, curve 2), two clear redox couples are observed. A small peak at E_{f1} = +0.08 ± 0.02 V and a more pronounced one at E_{f2} = +0.25 ± 0.05 V vs Ag/AgCl are consistent with leucoemeraldine to emeraldine and emeraldine to pernigraniline redox transitions, respectively, and are typical for sulfonated polyanilines.[44−47] The voltammetric behavior of PMSA1 on the macroITO electrode is very similar to that observed on the planar ITO;[43] however, the amount of the immobilized PMSA1 is much higher on the macroITO electrode compared to the flat one (see Materials and Methods).

The incorporation of the polymer can be clearly observed in the UV−vis spectra, which show a strong band at 469 nm assigned to a low-wavelength polaron band of the polyaniline emeraldine salt (ES) state.[42,46] The incorporation of the PQQ-GDH enzyme does not change the voltammetric behavior of
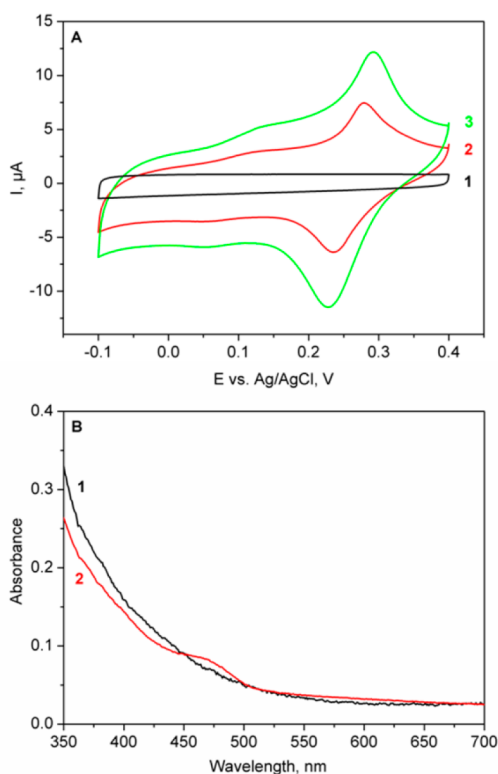
Figure 2. (A) Cyclic voltammograms for the (1) blank macroITO, (2) macroITO/PMSA1, and (3) macroITO/(PMSA1:PQQ-GDH) electrodes. (B) UV−vis spectra of the (1) blank macroITO and 2-macroITO/(PMSA1:PQQ-GDH) electrodes. Measurements were taken in a 20 mM MES + 5 mM CaCl$_2$ buffer at pH 6.

Figure 3. (A) Cyclic voltammograms and (B) UV−vis spectra of the macroITO/(PMSA1:PQQ-GDH) electrodes in the absence (1) and in the presence (2) of glucose. Measurements were taken in a 20 mM MES + 5 mM CaCl$_2$ buffer at pH 6.

the polymer matrix much. The entrapped PQQ-GDH enzyme does not show a direct electrochemical signal in the absence of the glucose substrate; however, its presence leads to a change in the charging properties resulting from the interaction of PQQ-GDH with the polymeric chains (Figure 2A, curves 2 and 3). Therefore, we assume that the polymer and PQQ-GDH can penetrate the porous electrode and the enzyme is immobilized by means of the polymer. It should be pointed out that the electrodes are considered to be fully loaded with adsorbed material after 2 h of incubation in a polymer/enzyme solution because no additional increase in the current density occurs upon an increase of the incubation times to 1 or 2 days.

UV−vis spectra of the blank macroITO and macroITO/(PMSA1:PQQ-GDH) electrodes are summarized in Figure 2B. The appearance of the strong band at 469 nm assigned to a low-wavelength polaron band of the polyaniline ES state[42,46] indicates the immobilized polymer/enzyme network on macroITO. The concentration of the enzyme is not sufficient to have impact on the polymer spectra. Further spectroscopic features from the polymer are difficult to resolve because the macroITO electrodes show a basic absorbance in the range below 450 nm (Figure 2B, curve 1).

Bioelectrochemical Oxidation of Glucose at the macroITO/(PMSA1:PQQ-GDH) Electrodes. Upon the addition of the glucose substrate to the buffer solution, the macroITO/(PMSA1:PQQ-GDH) electrode shows a significant bioelectrocatalytic current, giving proof of the presence of the electroactive enzyme in the film (Figure 3A). Control experiments without enzyme show no glucose conversion in this potential range. The catalytic current starts from a potential
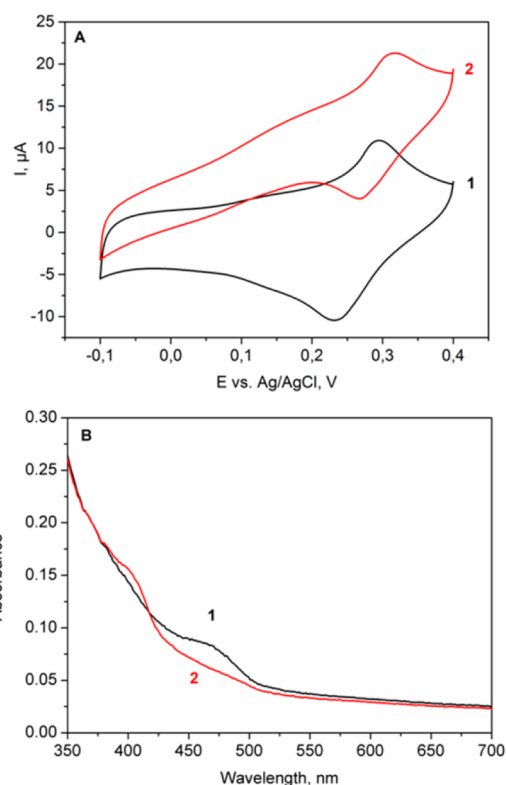
of about $E = -0.1$ V vs Ag/AgCl and reaches a change of $\Delta I = 13 \pm 3$ μA at $E = +0.35$ V, $n = 3$ (curve 2). Bioelectrocatalysis demonstrates efficient electron exchange between the redox center of the entrapped enzyme and the accessible porous conductive electrode surface, indicating that the polymer environment inside the macroITO pores ensures the catalytic activity of PQQ-GDH and allows efficient electron withdrawal from the reduced enzyme.

When we compare the catalytic current density of the macroporous PQQ-GDH electrode developed here with those of electrodes that have been constructed in a similar manner on flat ITO ($\Delta I = 57$ nA), a significant improvement of the bioelectrocatalytic properties of the system can be demonstrated. The catalytic currents for the same glucose concentration are increased by more than 2 orders of magnitude (~228-fold) by using macroITO electrodes. When one compares this enhancement with the electroactive area increase from flat ITO to porous macroITO—concluded from analysis of the voltammetric charging current in a pure buffer solution (see Materials and Methods), which gives about a 40-fold increase—it is obvious that not only the high surface within the macroITO structure but also the high polymer amount in combination with entrapment of the enzyme contribute to the drastically enhanced bioelectrocatalytic current. This is a clear achievement of the presented electrode, compared to other bioelectrocatalytic systems.[34]

In order to demonstrate application of the nanoporous system as an optical transducer, macroITO/(PMSA1:PQQ-GDH) electrodes have been measured by UV−vis in the presence and in the absence of substrate. Figure 3B demonstrates the spectral changes of the mixed polymer/

enzyme film on macroITO in the absence (curve 1) and in the presence (curve 2) of 5 mM glucose. According to the known redox-state-dependent spectral characteristics of PMSA1,[42,43,46] it can be seen that reduction of the polymer upon the addition of glucose occurs with the appearance of a characteristic band at 408 nm. Despite absorbance of macroITO itself in this wavelength range, the polymer change can be clearly verified and supports our electrochemical data, demonstrating that electron transfer between the entrapped PQQ-GDH and the surrounding polymer in the macroporous electrodes can be followed also by optical means.

The start potential for glucose oxidation of the enzyme electrode macroITO/(PMSA1:PQQ-GDH) is located near the redox potential of the enzyme. However, the question arises as to whether the electrons are transferred directly to the electrode surface or small amounts of free PQQ are acting as mediators,[48,49] because PQQ might be present in the polymer film or in the porous electrode as a result of partial denaturation of the holoenzyme during immobilization. To clarify this question, the macroITO/(PMSA1:PQQ-GDH) electrodes have been examined in the presence of 5 mM glucose with increasing concentration of free PQQ in solution. Figure 4
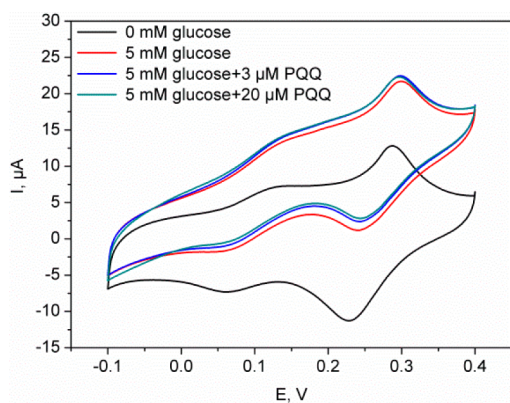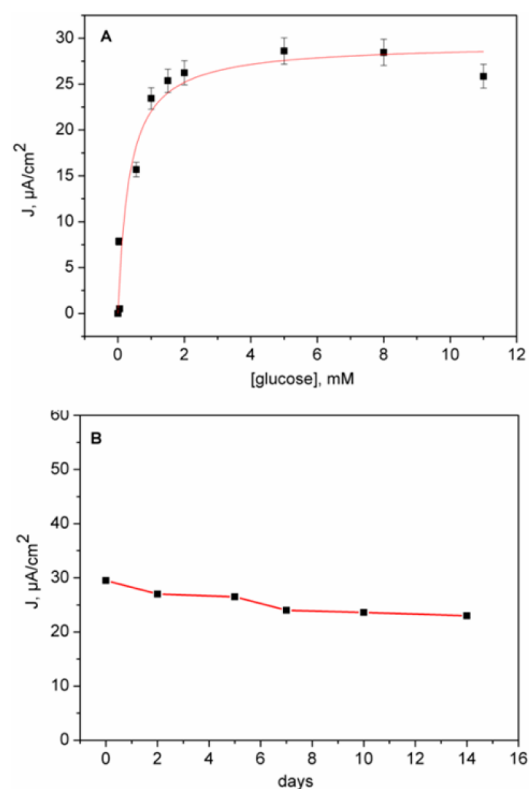

Figure 4. Cyclic voltammograms of the macroITO/(PMSA1:PQQ-GDH) electrode in solutions containing glucose and increasing amounts of free PQQ. Measurements were performed in a 20 mM MES + 5 mM CaCl$_2$ buffer at pH 6 and a scan rate of 5 mV s^{-1}.

demonstrates that even an amount of 20 μM PQQ, which is 4 times higher than the concentration of the enzyme during the entrapment process, does not cause any significant enhancement of the bioelectrocatalytic response. These measurements, together with the reconstitution procedure of the enzyme in which an excess of free PQQ with respect to the enzyme concentration is avoided, discard a hypothesis on the potential mediation of electron transfer by some denatured enzyme with liberated PQQ.

At this point, it is necessary to add some comments on the nature of electron transfer in the established polymer/enzyme electrode system. As one can see from Figure 4, the polymer is redox-active on the macroporous electrode. However, according to the formal potential of polymer conversions and the starting potential of bioelectrocatalysis, we conclude that its oxidation is not necessary to collect electrons from the reduced enzyme. This indicates that no mediation by the polymer takes place. Consequently, the conducting properties of sulfonated polyaniline have been exploited in this concept to drive electron transfer from the enzyme PQQ-GDH to the polymer-modified electrode. The polymer acts as an immobilization matrix,

holding and wiring the enzyme within the pores of macroITO electrodes.

Analytical Performance of the macroITO/(PMSA1:PQQ-GDH) Electrodes. Figure 5A shows the

Figure 5. (A) Change in the catalytic current density of the macroITO/(PMSA1:PQQ-GDH) electrode as a function of the glucose concentration. Bioelectrocatalytic signals were registered from the respective cyclic voltammograms at $E = +0.35$ V (surface area used for the calculation = 0.032 cm^2). (B) Stability of macroITO/(PMSA1:PQQ-GDH) at [glucose] = 5 mM. Measurements were performed in a 20 mM MES + 5 mM CaCl$_2$ buffer at pH 6 and a scan rate of 5 mV s^{-1}.

calibration curve obtained for macroITO/(PMSA1:PQQ-GDH) electrodes ($n = 3$). The oxidation current was determined as a function of the glucose concentration at $E = +0.35$ V vs Ag/AgCl. The current follows the glucose concentration in the range from 0.025 to 2 mM and reaches saturation at 5−10 mM. An apparent K_m value of 0.33 mM glucose has been calculated, which is considerably smaller than the intrinsic K_m of soluble GDH in solution (~45 mM);[50−53] nevertheless, it fits into the range of apparent K_m (0.1−5 mM) on some modified electrodes.[54−58] This shows that, besides enzyme kinetics, electron transfer, together with the accessibility of the enzyme's active center toward the substrate, are important factors for the behavior of the whole system. It has to be explicitly noted here that glucose detection can be performed at much lower potential because bioelectrocatalysis already starts at −0.1 V vs Ag/AgCl. This is advantageous in complex media, in which other redox-active substances are present.

Because long-term stability is an exceptionally important parameter for evaluation of the performance of a detection system, we have traced the stability of our macroITO/(PMSA1:PQQ-GDH) electrodes by testing their activity in a

glucose solution, after the electrodes were kept at 4 °C in 20 mM MES + 5 mMCaCl$_2$, pH 6, when not in use. Figure 5B shows that the catalytic current response maintained over 90% of the initial value after 12 days. This is significant progress compared to other kinds of PQQ-GDH immobilization procedures, resulting in substantial activity loss already during the first week, and demonstrates that the entrapment of PQQ-GDH in the sulfonated polyaniline films within the macroporous electrodes leads to an improved retainment of activity. Additionally, it has to be mentioned here that no intermittent treatment of the electrodes with PQQ has been performed, demonstrating that the environment in the 3D structure is well adapted to the enzyme. The high stability makes this type of architecture promising for consideration as a candidate for the construction of enzyme-based biosensors.

■ CONCLUSION

In summary, we have demonstrated an efficient platform for the entrapment of PQQ-GDH by fabricating a polymer/enzyme network inside the pores of macroITO. MacroITO has been shown to represent a suitable 3D electrode matrix for the incorporation of sulfonated polyaniline and PQQ-GDH, taking advantage of a pore size that does not limit immobilization of large amounts of enzyme in an active form. The amount of bound polymer within the macroporous electrodes is high enough to observe electrochemical signals and spectroscopic signatures. The large inner surface area of the material is well accessible for enzyme and substrate because a tremendously enhanced bioelectrocatalytic response in comparison with those of flat Au and ITO electrodes is observed. Bioelectrocatalysis starts near the potential of the enzyme redox center; i.e., no large overpotential is needed to drive the reaction. In particular, the mild fabrication process and the active role of the polymer film in closing the enzymatic cycle (i.e., withdrawing electrons from the reduced biomolecule) lead to a system with high stability because efficient bioelectrocatalysis can be detected even after more than 12 days in permanent electrolyte contact. We envision that the combination of the 3D porous electrode structure with a conductive polymer and an enzyme can be used for the development of many bioanalytical devices that combine optical and electrochemical detection for application in health care or environmental monitoring.

■ MATERIALS AND METHODS

Chemicals. MES [2-(N-morpholino)ethanesulfonic acid] buffer was purchased from Sigma-Aldrich (Taufkirchen, Germany), and dehydrated calcium chloride and anhydrous D-glucose were obtained from Fluka Analytics (Taufkirchen, Germany). They were used without further purification. Poly(2-methoxyaniline-5-sulfonic acid)-co-aniline polymer (PMSA1; Scheme 1) was synthesized as reported before.[42,59] sGDH (Acinetobacter calcoaceticus) was a kind gift from Roche Diagnostics GmbH. The enzyme was recombinantly expressed in Escherichia coli. PQQ was purchased from Wako Pure Chemical Industries. 18 MΩ Millipore water (Eschborn, Germany) was used for all types of measurements.

Preparation of Nanostructured macroITO Films. Porous ITO electrodes used in this work were prepared by a direct coassembly of poly(methyl methacrylate) (PMMA) beads and indium tin hydroxide nanoparticles (nano-ITOH) as described before.[26] In brief, PMMA beads with a diameter of 370 nm were synthesized according to an emulsion polymerization route.[60,61] Indium tin hydroxide nanoparticles were prepared by a solvothermal procedure.[27] In a typical synthesis of nano-ITOH, tin(IV) chloride pentahydrate (Aldrich; 0.122 g, 0.35 mmol) was added to a clear solution of indium(III) chloride (Aldrich; 0.698 g, 3.16 mmol) in 7 mL of ethylene glycol

(Aldrich; ≥99%, used without further drying). The molar ratio of tin and indium was 1:9 (mol:mol). Separately, 0.420 g of sodium hydroxide (Aldrich; 97%) was dissolved in 7 mL of ethylene glycol. Both solutions were combined at 0 °C, stirred for another 15 min, and transferred into a glass-lined autoclave, which was kept in a laboratory oven preheated at 205 °C for 24 h. The formed product was separated by centrifugation (47800 rcf for 20 min), washed once in ca. 14 mL of bidistilled water (manual stirring), and centrifuged again at 47800 rcf for 20 min. The water should be decanted immediately after centrifugation to prevent redispersion of ITOH nanoparticles.

For the fabrication of macroporous films, still wet nano-ITOH (300 mg) containing 100 mg of dry inorganic content was dispersed in 0.75 mL of water (Millipore Q grade), stirred at room temperature until the colloidal solution turned transparent or slightly opaque, and ultrasonicated for 30 min. Separately, an aqueous colloidal PMMA suspension (15 wt %) was stirred for 1 h and ultrasonicated for 30 min. The amount of PMMA beads was calculated from the weight of nano-ITOH (dry content) as 3 weight parts of PMMA to 1 weight part of ITOH; in this example, it corresponds to 2 mL of 15 wt % PMMA dispersion. Finally, hydroxypropylcellulose (HPC; MW ca. 100000, from Sigma-Aldrich) was added to a combined solution of PMMA and nano-ITOH, stirred together for 3–4 h, and ultrasonicated for 30 min. The amount of cellulose corresponds to 10 wt % of the PMMA beads; in this example, it is 30 mg of HPC in a total volume of 3 mL, which corresponds to 1 wt % HPC. The homogeneous dispersion was dip-coated three times on planar ITO substrates at a dip-coating rate of 0.63 mm s^{-1} with a drying step at 80 °C for 45 min after each coating. The relative humidity and temperature in the coating chamber were 35% and 20 °C, respectively. The films were finally calcined in air at 400 °C (achieved with a ramp of 13 °C min^{-1}) for 30 min. To improve the electrical conductivity of the ITO layers, they were additionally heated in forming gas (composed of 5% hydrogen and 95% nitrogen) at 400 °C (achieved with a ramp of 2 °C min^{-1}) for 30 min.

Preparation of the Enzyme Solution. sGDH was dissolved in 5 mM MES buffer in the presence of 1 mM CaCl$_2$, and the pH was adjusted to 5. apoGDH was reconstituted by a PQQ-GDH ratio of 1 according to Olsthoorn and Duine.[62] For this purpose, sGDH and PQQ were incubated together for 1 h at room temperature in the dark. Aliquots were stored at −20 °C. Prior to each measurement, the specific activity of the reconstituted enzyme was determined to be 2200 ± 30 U mg^{-1} by using 2,6-dichlorophenolindophenol as an electron acceptor.

Construction of Polymer/Enzyme Films. For the preparation of polymer/enzyme films, the previously cleaned rectangular ITO-coated glass slides with a surface resistivity of 15−25 Ω sq^{-1} (obtained from Sigma-Aldrich, Taufkirchen, Germany) and nanostructured ITO were initially incubated in buffer solutions of the PMSA1:PQQ-GDH mixture (1.5 mg mL^{-1} PMSA1; 5 μM PQQ-GDH; 20 mM MES + 5 mM CaCl$_2$; pH 6) in darkness for 2 h. Afterward, the PMSA1:PQQ-GDH electrode was dipped into the same buffer without enzyme and polymer to wash away the unbound material.

Instruments and Characterization Methods. Film characterization by SEM was performed on a JEOL JSM-6500F scanning electron microscope equipped with a field-emission gun at 10 kV. Bright-field and high-resolution TEM as well as scanning TEM in high-angle annular dark-field mode were carried out using a field-emission FEI Titan 80-300 operated at 300 kV.

Electrochemical measurements were performed at room temperature in a homemade 1 mL cell using an Ag/AgCl/1 M KCl reference (Biometra, Germany) and a platinum wire counter electrode. Cyclic voltammetric experiments were carried out with a μAutolab Type II device (Metrohm, The Netherlands). The scan rate was set to 5 mV s^{-1}. The potential range was chosen as between −0.4 and +0.4 V vs Ag/AgCl. Data analysis was performed using GPES software (General Purpose for Electrochemical System, Eco Chemie, The Netherlands). UV−vis measurements were carried out using an Evolution 300 spectrophotometer (Thermo Fischer Scientific, Germany).

The amount of immobilized polymer was compared by integration of voltammetric peaks measured on both flat ITO + polymer[43] and

macroITO + polymer electrodes under the same experimental conditions (20 mM MES + 5 mM CaCl$_2$; pH 6; scan rate of −5 mV s^{-1}). The electroactive area increase of the macroITO with respect to the flat ITO was estimated by comparing the charging current of both electrodes in CV measurements at a scan rate of 50 mV/s vs Ag/AgCl.

■ AUTHOR INFORMATION

Corresponding Authors
*E-mail: david.sarauli@th-wildau.de.
*E-mail: flisdat@th-wildau.de.

Author Contributions
The manuscript was written through contributions of all authors. All authors have given approval to the final version of the manuscript.

Notes
The authors declare no competing financial interest.

■ REFERENCES

(1) Cracknell, J. A.; Vincent, K. A.; Armstrong, F. A. Enzymes as Working or Inspirational Electrocatalysts for Fuel Cells and Electrolysis. *Chem. Rev.* **2008**, *108*, 2439−2461.

(2) Leger, C.; Bertrand, P. Direct Electrochemistry of Redox Enzymes as a Tool for Mechanistic Studies. *Chem. Rev.* **2008**, *108*, 2379−2438.

(3) Lisdat, F.; Dronov, R.; Mohwald, H.; Scheller, F. W.; Kurth, D. G. Self-Assembly of Electro-Active Protein Architectures on Electrodes for the Construction of Biomimetic Signal Chains. *Chem. Commun.* **2009**, 274−283.

(4) Ludwig, R.; Ortiz, R.; Schulz, C.; Harreither, W.; Sygmund, C.; Gorton, L. Cellobiose Dehydrogenase Modified Electrodes: Advances by Materials Science and Biochemical Engineering. *Anal. Bioanal. Chem.* **2013**, *405*, 3637−3658.

(5) Noll, T.; Noll, G. Strategies for "Wiring" Redox-Active Proteins to Electrodes and Applications in Biosensors, Biofuel Cells, and Nanotechnology. *Chem. Soc. Rev.* **2011**, *40*, 3564−3576.

(6) Shleev, S.; Tkac, J.; Christenson, A.; Ruzgas, T.; Yaropolov, A. I.; Whittaker, J. W.; Gorton, L. Direct Electron Transfer between Copper-Containing Proteins and Electrodes. *Biosens. Bioelectron.* **2005**, *20*, 2517−2554.

(7) Tkac, J.; Svitel, J.; Vostiar, I.; Navratil, M.; Gemeiner, P. Membrane-Bound Dehydrogenases from Gluconobacter Sp.: Interfacial Electrochemistry and Direct Bioelectrocatalysis. *Bioelectrochemistry* **2009**, *76*, 53−62.

(8) Hanefeld, U.; Gardossi, L.; Magner, E. Understanding Enzyme Immobilisation. *Chem. Soc. Rev.* **2009**, *38*, 453−468.

(9) Rodrigues, R. C.; Ortiz, C.; Berenguer-Murcia, A.; Torres, R.; Fernandez-Lafuente, R. Modifying Enzyme Activity and Selectivity by Immobilization. *Chem. Soc. Rev.* **2013**, *42*, 6290−6307.

(10) Secundo, F. Conformational Changes of Enzymes upon Immobilisation. *Chem. Soc. Rev.* **2013**, *42*, 6250−6261.

(11) Sheldon, R. A.; van Pelt, S. Enzyme Immobilisation in Biocatalysis: Why, What and How. *Chem. Soc. Rev.* **2013**, *42*, 6223−6235.

(12) Cherry, R. J.; Bjornsen, A. J.; Zapien, D. C. Direct Electron Transfer of Ferritin Adsorbed at Tin-Doped Indium Oxide Electrodes. *Langmuir* **1998**, *14*, 1971−1973.

(13) Dhand, C.; Das, M.; Sumana, G.; Srivastava, A. K.; Pandey, M. K.; Kim, C. G.; Datta, M.; Malhotra, B. D. Preparation, Characterization and Application of Polyaniline Nanospheres to Biosensing. *Nanoscale* **2010**, *2*, 747−754.

(14) El Kasmi, A.; Leopold, M. C.; Galligan, R.; Robertson, R. T.; Saavedra, S. S.; El Kacemi, K.; Bowden, E. F. Adsorptive Immobilization of Cytochrome C on Indium/Tin Oxide (ITO): Electrochemical Evidence for Electron Transfer-Induced Conformational Changes. *Electrochem. Commun.* **2002**, *4*, 177−181.

(15) Fang, A. P.; Ng, H. T.; Li, S. F. Y. A High-Performance Glucose Biosensor Based on Monomolecular Layer of Glucose Oxidase Covalently Immobilised on Indium−Tin Oxide Surface. *Biosens. Bioelectron.* **2003**, *19*, 43−49.

(16) Yagati, A. K.; Lee, T.; Min, J.; Choi, J. W. An Enzymatic Biosensor for Hydrogen Peroxide Based on CeO$_2$ Nanostructure Electrodeposited on ITO Surface. *Biosens. Bioelectron.* **2013**, *47*, 385−390.

(17) Cantale, V.; Simeone, F. C.; Gambari, R.; Rampi, M. A. Gold Nano-Islands on FTO as Plasmonic Nanostructures for Biosensors. *Sens. Actuators, B* **2011**, *152*, 206−213.

(18) Lamberti, F.; Agnoli, S.; Brigo, L.; Granozzi, G.; Giomo, M.; Elvassore, N. Surface Functionalization of Fluorine-Doped Tin Oxide Samples through Electrochemical Grafting. *ACS Appl. Mater. Interfaces* **2013**, *5*, 12887−12894.

(19) Lavanya, N.; Radhakrishnan, S.; Sekar, C. Fabrication of Hydrogen Peroxide Biosensor Based on Ni Doped SnO$_2$ Nanoparticles. *Biosens. Bioelectron.* **2012**, *36*, 41−47.

(20) Saha, S.; Tomar, M.; Gupta, V. Fe Doped ZnO Thin Film for Mediator-Less Biosensing Application. *J. Appl. Phys.* **2012**, *111*, 102804.

(21) Wang, P.; Li, S. Q.; Kan, J. Q. A Hydrogen Peroxide Biosensor Based on Polyaniline/FTO. *Sens. Actuators, B* **2009**, *137*, 662−668.

(22) Aksu, Y.; Frasca, S.; Wollenberger, U.; Driess, M.; Thomas, A. A Molecular Precursor Approach to Tunable Porous Tin-Rich Indium Tin Oxide with Durable High Electrical Conductivity for Bioelectronic Devices. *Chem. Mater.* **2012**, *23*, 1798−1804.

(23) Buonsanti, R.; Pick, T. E.; Krins, N.; Richardson, T. J.; Helms, B. A.; Milliron, D. J. Assembly of Ligand-Stripped Nanocrystals into Precisely Controlled Mesoporous Architectures. *Nano Lett.* **2012**, *12*, 3872−3877.

(24) Frasca, S.; von Graberg, T.; Feng, J. J.; Thomas, A.; Smarsly, B. M.; Weidinger, I. M.; Scheller, F. W.; Hildebrandt, P.; Wollenberger, U. Mesoporous Indium Tin Oxide as a Novel Platform for Bioelectronics. *ChemCatChem* **2010**, *2*, 839−845.

(25) Hamd, W.; Chavarot-Kerlidou, M.; Fize, J.; Muller, G.; Leyris, A.; Matheron, M.; Courtin, E.; Fontecave, M.; Sanchez, C.; Artero, V.; Laberty-Robert, C. Dye-Sensitized Nanostructured Crystalline Mesoporous Tin-Doped Indium Oxide Films with Tunable Thickness for Photoelectrochemical Applications. *J. Mater. Chem. A* **2013**, *1*, 8217−8225.

(26) Liu, Y.; Peters, K.; Mandlmeier, B.; Müller, A.; Fominykh, K.; Rathousky, J.; Scheu, C.; Fattakhova-Rohlfing, D. Macroporous Indium Tin Oxide Electrode Layers as Conducting Substrates for Immobilization of Bulky Electroactive Guests. *Electrochim. Acta* **2014**, *140*, 108−115.

(27) Liu, Y. J.; Stefanic, G.; Rathousky, J.; Hayden, O.; Bein, T.; Fattakhova-Rohlfing, D. Assembly of Mesoporous Indium Tin Oxide Electrodes from Nano-Hydroxide Building Blocks. *Chem. Sci.* **2012**, *3*, 2367−2374.

(28) Schaming, D.; Renault, C.; Tucker, R. T.; Lau-Truong, S.; Aubard, J.; Brett, M. J.; Balland, V.; Limoges, B. Spectroelectrochemical Characterization of Small Hemoproteins Adsorbed within Nanostructured Mesoporous ITO Electrodes. *Langmuir* **2012**, *28*, 14065−14072.

(29) Hou, K.; Puzzo, D.; Helander, M. G.; Lo, S. S.; Bonifacio, L. D.; Wang, W.; Lu, Z.-H.; Scholes, G. D.; Ozin, G. A. Dye-Anchored Mesoporous Antimony-Doped Tin Oxide Electrochemiluminescence Cell. *Adv. Mater.* **2009**, *21*, 2492−2496.

(30) Frasca, S.; Richter, C.; von Graberg, T.; Smarsly, B. M.; Wollenberger, U. Electrochemical Switchable Protein-Based Optical Device. *Eng. Life Sci.* **2011**, *11*, 554−558.

(31) Kwan, P.; Schmitt, D.; Volosin, A. M.; McIntosh, C. L.; Seo, D. K.; Jones, A. K. Spectroelectrochemistry of Cytochrome C and Azurin Immobilized in Nanoporous Antimony-Doped Tin Oxide. *Chem. Commun.* **2011**, *47*, 12367−12369.

(32) Müller, V.; Rathousky, J.; Fattakhova-Rohlfing, D. Covalent Immobilization of Redox Protein within the Mesopores of Transparent Conducting Electrodes. *Electrochim. Acta* **2014**, *116*, 1−8.

(33) Reipa, V.; Mayhew, M. P.; Vilker, V. L. A Direct Electrode-Driven P450 Cycle for Biocatalysis. *Proc. Natl. Acad. Sci. U. S. A.* **1997**, *94*, 13554−13558.

(34) Frasca, S.; Milan, A. M.; Guiet, A.; Goebel, C.; Perez-Caballero, F.; Stiba, K.; Leimkuhler, S.; Fischer, A.; Wollenberger, U. Bioelectrocatalysis at Mesoporous Antimony Doped Tin Oxide Electrodes—Electrochemical Characterization and Direct Enzyme Communication. *Electrochim. Acta* **2013**, *110*, 172−180.

(35) Leech, D.; Kavanagh, P.; Schuhmann, W. Enzymatic Fuel Cells: Recent Progress. *Electrochim. Acta* **2012**, *84*, 223−234.

(36) Rubenwolf, S.; Kerzenmacher, S.; Zengerle, R.; von Stetten, F. Strategies to Extend the Lifetime of Bioelectrochemical Enzyme Electrodes for Biosensing and Biofuel Cell Applications. *Appl. Microbiol. Biotechnol.* **2011**, *89*, 1315−1322.

(37) Zayats, M.; Willner, B.; Willner, I. Design of Amperometric Biosensors and Biofuel Cells by the Reconstitution of Electrically Contacted Enzyme Electrodes. *Electroanalysis* **2008**, *20*, 583−601.

(38) Katz, E.; MacVittie, K. Implanted Biofuel Cells Operating in Vivo—Methods, Applications and Perspectives—Feature Article. *Energy Environ. Sci.* **2013**, *6*, 2791−2803.

(39) Southcott, M.; MacVittie, K.; Halamek, J.; Halamkova, L.; Jemison, W. D.; Lobel, R.; Katz, E. A. Pacemaker Powered by an Implantable Biofuel Cell Operating under Conditions Mimicking the Human Blood Circulatory System—Battery Not Included. *Phys. Chem. Chem. Phys.* **2013**, *15*, 6278−6283.

(40) Scherbahn, V.; Putze, M. T.; Dietzel, B.; Heinlein, T.; Schneider, J. J.; Lisdat, F. Biofuel Cells Based on Direct Enzyme-Electrode Contacts Using PQQ-Dependent Glucose Dehydrogenase/Bilirubin Oxidase and Modified Carbon Nanotube Materials. *Biosens. Bioelectron.* **2014**, *61*, 631−638.

(41) Strack, G.; Nichols, R.; Atanassov, P.; Luckarift, H. R.; Johnson, G. R. Modification of Carbon Nanotube Electrodes with 1-Pyrenebutanoic Acid, Succinimidyl Ester for Enhanced Bioelectrocatalysis. *Methods Mol. Biol. (N. Y.)* **2013**, *1051*, 217−228.

(42) Sarauli, D.; Xu, C. G.; Dietzel, B.; Schulz, B.; Lisdat, F. Differently Substituted Sulfonated Polyanilines: The Role of Polymer Compositions in Electron Transfer with Pyrroloquinoline Quinone-Dependent Glucose Dehydrogenase. *Acta Biomater.* **2013**, *9*, 8290−8298.

(43) Sarauli, D.; Xu, C.; Dietzel, B.; Schulz, B.; Lisdat, F. A Multilayered Sulfonated Polyaniline Network with Entrapped Pyrroloquinoline Quinone-Dependent Glucose Dehydrogenase: Tunable Direct Bioelectrocatalysis. *J. Mater. Chem. B* **2014**, *2*, 3196−3203.

(44) Dennany, L.; Innis, P. C.; McGovern, S. T.; Wallace, G. G.; Forster, R. J. Electronic Interactions within Composites of Polyanilines Formed under Acidic and Alkaline Conditions. Conductivity, ESR, Raman, UV−Vis and Fluorescence Studies. *Phys. Chem. Chem. Phys.* **2011**, *13*, 3303−3310.

(45) Masdarolomoor, F.; Innis, P. C.; Wallace, G. G. Electrochemical Synthesis and Characterisation of Polyaniline/Poly(2-Methoxyaniline-5-Sulfonic Acid) Composites. *Electrochim. Acta* **2008**, *53*, 4146−4155.

(46) Pornputtkul, Y.; Strounina, E. V.; Kane-Maguire, L. A. P.; Wallace, G. G. Redox Behavior of Poly(2-Methoxyaniline-5-Sulfonic Acid) and Its Remarkable Thermochromism, Solvatochromism, and Ionochromism. *Macromolecules* **2010**, *43*, 9982−9989.

(47) Sanchis, C.; Ghanem, M. A.; Salavagione, H. J.; Morallon, E.; Bartlett, P. N. The Oxidation of Ascorbate at Copolymeric Sulfonated Poly(Aniline) Coated on Glassy Carbon Electrodes. *Bioelectrochemistry* **2011**, *80*, 105−113.

(48) Jin, W.; Wollenberger, U.; Scheller, F. W. PQQ as Redox Shuttle for Quinoprotein Glucose Dehydrogenase. *Biol. Chem.* **1998**, *379*, 1207−1211.

(49) Karyakin, A. A. Principles of Direct (Mediator Free) Bioelectrocatalysis. *Bioelectrochemistry* **2012**, *88*, 70−75.

(50) Dokter, P.; Frank, J.; Duine, J. A. Purification and Characterization of Quinoprotein Glucose-Dehydrogenase from Acinetobacter Calcoaceticus L.M.D. 79.41. *Biochem. J.* **1986**, *239*, 163−167.

(51) Durand, F.; Stines-Chaumeil, C.; Flexer, V.; Andre, I.; Mano, N. Designing a Highly Active Soluble PQQ-Glucose Dehydrogenase for Efficient Glucose Biosensors and Biofuel Cells. *Biochem. Biophys. Res. Commun.* **2010**, *402*, 750−754.

(52) Flexer, V.; Durand, F.; Tsujimura, S.; Mano, N. Efficient Direct Electron Transfer of PQQ-Glucose Dehydrogenase on Carbon Cryogel Electrodes at Neutral Ph. *Anal. Chem.* **2011**, *83*, 5721−5727.

(53) Matsushita, K.; Shinagawa, E.; Adachi, O.; Ameyama, M. Quinoprotein D-Glucose Dehydrogenase of the Acinetobacter Calcoaceticus Respiratory-Chain—Membrane-Bound and Soluble Forms Are Different Molecular-Species. *Biochemistry* **1989**, *28*, 6276−6280.

(54) Flexer, V.; Mano, N. Wired Pyrroloquinoline Quinone Soluble Glucose Dehydrogenase Enzyme Electrodes Operating at Unprecedented Low Redox Potential. *Anal. Chem.* **2014**, *86*, 2465−2473.

(55) Gobel, G.; Schubart, I. W.; Scherbahn, V.; Lisdat, F. Direct Electron Transfer of PQQ-Glucose Dehydrogenase at Modified Carbon Nanotubes Electrodes. *Electrochem. Commun.* **2011**, *13*, 1240−1243.

(56) Ivnitski, D.; Atanassov, P.; Apblett, C. Direct Bioelectrocatalysis of PQQ-Dependent Glucose Dehydrogenase. *Electroanalysis* **2007**, *19*, 1562−1568.

(57) Malinauskas, A.; Kuzmarskyte, J.; Meskys, R.; Ramanavicius, A. Bioelectrochemical Sensor Based on PQQ-Dependent Glucose Dehydrogenase. *Sens. Actuators, B* **2004**, *100*, 387−394.

(58) Strack, G.; Babanova, S.; Farrington, K. E.; Luckarift, H. R.; Atanassov, P.; Johnson, G. R. Enzyme-Modified Buckypaper for Bioelectrocatalysis. *J. Electrochem. Soc.* **2013**, *160*, G3178−G3182.

(59) Sarauli, D.; Xu, C. G.; Dietzel, B.; Stiba, K.; Leimkuhler, S.; Schulz, B.; Lisdat, F. Thin Films of Substituted Polyanilines: Interactions with Biomolecular Systems. *Soft Matter* **2012**, *8*, 3848−3855.

(60) Mandlmeier, B.; Minar, N. K.; Feckl, J. M.; Fattakhova-Rohlfing, D.; Bein, T. Tuning the Crystallinity Parameters in Macroporous Titania Films. *J. Mater. Chem. A* **2014**, *2*, 6504−6511.

(61) Mandlmeier, B.; Szeifert, J. M.; Fattakhova-Rohlfing, D.; Amenitsch, H.; Bein, T. Formation of Interpenetrating Hierarchical Titania Structures by Confined Synthesis in Inverse Opal. *J. Am. Chem. Soc.* **2011**, *133*, 17274−17282.

(62) Olsthoorn, A. J. J.; Duine, J. A. Production, Characterization, and Reconstitution of Recombinant Quinoprotein Glucose Dehydrogenase (Soluble Type; EC 1.1.99.17) Apoenzyme of Acinetobacter Calcoaceticus. *Arch. Biochem. Biophys.* **1996**, *336*, 42−48.